

Collisionless kinetic-fluid closure and its application to the three-mode ion temperature gradient driven system

H. Sugama and T.-H. Watanabe

National Institute for Fusion Science, Japan and Graduate University for Advanced Studies, Toki, Gifu 509-5292, Japan

W. Horton

Institute for Fusion Studies, The University of Texas at Austin, Austin, Texas 78712

(Received 22 September 2000; accepted 28 February 2001)

A novel closure model is presented to give a set of fluid equations which describe a collisionless kinetic system. In order to take account of the time reversal symmetry of the collisionless kinetic equation, the new closure model relates the parallel heat flux to the temperature and the parallel flow in terms of the real-valued coefficients in the unstable wave number space. Effects of the closure model on turbulence saturation and anomalous transport are investigated based on kinetic and fluid entropy balances. When the closure model is applied to the three-mode ion temperature gradient (ITG) driven system, the fluid system of equations reproduces the exact nonlinear kinetic solution found by Watanabe, Sugama, and Sato [Phys. Plasmas **7**, 984 (2000)]. Oscillatory behaviors and initial amplitude dependence of other numerical kinetic solutions of the three-mode ITG problem can also be accurately described by the fluid system. © 2001 American Institute of Physics. [DOI: 10.1063/1.1367319]

I. INTRODUCTION

Many theoretical studies have been done in order to understand anomalous transport processes observed in magnetically confined plasmas. Recently, predictions of the anomalous transport coefficients have come to be made by first-principle simulations of the ion temperature gradient (ITG) turbulence¹ based on gyrokinetic^{2–5} and gyrofluid^{6–9} (or gyro-Landau-fluid) models. Gyrokinetic simulations directly solve gyrokinetic equations for gyrocenter distribution functions and the Maxwell equations for electromagnetic fields while gyrofluid simulations solve a truncated system of fluid equations instead of the gyrokinetic equation. The gyrofluid simulations are attractive in that less computer memory and time are consumed although they depend on a closure relation between the highest-order fluid variable and lower-order variables which is assumed to be valid even for collisionless kinetic systems. Since conventional gyrofluid closure models^{10,11} are derived so as to accurately reproduce kinetic dispersion relations for linear modes, the gyrokinetic and gyrofluid simulations show good agreements in their linear results. However, there exist disagreements in their nonlinear results such as the saturated fluctuation levels and the turbulent transport coefficients.^{12,13}

The three-mode ITG system² is one of the simplest examples to show these agreements and disagreements between the kinetic and Landau-fluid models, in which effects of finite gyroradii are neglected by taking the long-wavelength limit. Recently, an exact nonlinear solution of the three-mode ITG problem was found by Watanabe, Sugama, and Sato (WSS).¹⁴ The nonlinear solution of the three-mode ITG problem shows periodic oscillation of the amplitude of the electrostatic potential. On the other hand, the solution of the kinetic-fluid equations using the conventional linear closure

models fail to reproduce this oscillation and instead give the amplitude saturation at a certain value.¹⁵ Also, it is important to note that the exact kinetic solution is symmetric in time reversal while the solution of the conventional kinetic-fluid equations is not symmetric due to the dissipative closure term.

In this paper, a novel collisionless kinetic-fluid closure model is presented, which takes into account the time reversal symmetry of the collisionless kinetic equation by including nondissipative closure terms. It is shown that, when the new closure model is applied to the three-mode ITG problem, the exact kinetic solution by WSS is reproduced as a solution of the fluid equations. Recently, Mator and Parker presented a nonlinear closure model,¹⁵ which also describes the behavior of the WSS solution better than the conventional linear closure models. However, their model contains complicated procedures for analytical continuation of the plasma dispersion function with matrix arguments including nonlinear effects and it cannot be easily extended to systems with more than three modes. Our closure model does not contain such fundamental difficulties for application to systems with a large number of degrees of freedom. Another nonlinear closure model based on the phase velocity transform (PVT) was presented by Mator.¹⁶ As written in Ref. 17, one difficulty with the original PVT closure is that calculating the transform into the phase velocity space can be nearly as time-consuming as the original kinetic equation. Therefore, Mator proposed a Wentzel–Kramers–Brillouin (WKB)-type local approximation to make the PVT closure model more tractable.^{17,18} In this local PVT model as well as in all other closure models except for the original PVT model and ours, it is assumed that, for the wave number vector \mathbf{k} , the distribution function is written as $f_{\mathbf{k}}(v_{\parallel})$

$\times \exp(-i\omega_{\mathbf{k}}t + i\mathbf{k} \cdot \mathbf{x})$ with a single dominant complex-valued frequency $\omega_{\mathbf{k}}$. However, we show that, in the nonlinear stage with the time reversal symmetry, a complex-conjugate pair of functions $f_{\mathbf{k}}(v_{\parallel})$ and $f_{\mathbf{k}}^*(v_{\parallel})$ corresponding to $\omega_{\mathbf{k}}$ and $\omega_{\mathbf{k}}^*$ are required to describe the distribution function for each \mathbf{k} , which is what our closure model attempts to describe.

The collisionless turbulent system is also an interesting subject from the nonequilibrium thermodynamical point of view. In the collisionless system, an increase rate of the entropy functional defined in terms of the kinetic distribution function is equal to the product of transport fluxes and thermodynamic forces. Thus, no turbulent transport occurs in the collisionless steady state, or the entropy grows indefinitely in time for the transport fluxes to take finite nonzero values. This is called the *entropy paradox* by Krommes and Hu.¹⁹ In order to examine effects of the kinetic-fluid closure on the turbulence saturation and the anomalous transport, it is significantly useful to consider kinetic and fluid entropy balances.^{19–21} This thermodynamic aspect of the collisionless closure model is also discussed in the present work.

The rest of this work is organized as follows. In Sec. II, the new closure model is presented to give a closed set of fluid equations, which describe the collisionless system governed by the drift kinetic equation for ions, the adiabatic condition for electrons, and quasineutrality. When there exists a linearly unstable normal mode solution of the collisionless system, its complex conjugate also becomes a linear solution due to the time reversal symmetry. Our closure model is derived in order to express the parallel heat flux in terms of the temperature and the parallel flow for the normal mode as well as for the complex-conjugate mode. Also, the role of the closure model in the turbulence saturation and the anomalous transport is investigated based on the kinetic and fluid entropy balance equations. Application of the closure model to the three-mode ITG problem is given in Sec. III. The fluid system of equations with our model used can reproduce the exact nonlinear kinetic solution by WSS. It is also shown that oscillatory behaviors and initial amplitude dependence of other numerical kinetic solutions can be accurately described by the fluid system. Finally, conclusions are given in Sec. IV.

II. COLLISIONLESS KINETIC-FLUID CLOSURE

A. Basic equations

Let us start from the drift kinetic equation for ions with the mass m_i and the charge e in a slab geometry

$$\frac{\partial f}{\partial t} + v_{\parallel} \mathbf{b} \cdot \nabla f + \mathbf{v}_E \cdot \nabla f + \frac{e}{m_i} E_{\parallel} \frac{\partial f}{\partial v_{\parallel}} = 0, \quad (1)$$

where $f = f(\mathbf{x}, v_{\parallel}, t)$ is the ion distribution function integrated over the velocity \mathbf{v}_{\perp} perpendicular to the magnetic-field $\mathbf{B} \equiv B\mathbf{b}$, $v_{\parallel} \equiv \mathbf{v} \cdot \mathbf{b}$ is the parallel velocity, $E_{\parallel} \equiv \mathbf{E} \cdot \mathbf{b}$ is the parallel electric field, and $\mathbf{v}_E = c\mathbf{E} \times \mathbf{B}/B^2$ is the $\mathbf{E} \times \mathbf{B}$ drift velocity. The long perpendicular wavelength limit ($k_{\perp} \rho_i \ll 1$) is assumed in Eq. (1). We assume that the magnetic-field \mathbf{B} is uniform and constant. The electric field is written in terms of the electrostatic potential ϕ as $\mathbf{E} = -\nabla \phi$. The distribution function is given by the sum of a background Maxwellian

part $F_M = n_0(m_i/2\pi T_i)^{1/2} \exp(-m_i v^2/2T_i)$ and a perturbation part \tilde{f} , where n_0 and T_i denote the background density and temperature, respectively, which depend only on a coordinate x in the perpendicular direction.

We assume the adiabatic electron response. Then, the quasineutrality condition is written as

$$\int \tilde{f} dv_{\parallel} = n_0 \frac{e\phi}{T_e}. \quad (2)$$

Equations (1) and (2) form a closed system of equations to determine \tilde{f} and ϕ .

Now, we represent \tilde{f} and ϕ in terms of the Fourier expansion as

$$\tilde{f}(\mathbf{x}, v_{\parallel}, t) = \sum_{\mathbf{k}} f_{\mathbf{k}}(v_{\parallel}, t) e^{i\mathbf{k} \cdot \mathbf{x}}, \quad \phi(\mathbf{x}, t) = \sum_{\mathbf{k}} \phi_{\mathbf{k}}(t) e^{i\mathbf{k} \cdot \mathbf{x}}. \quad (3)$$

The drift kinetic equation (1) is rewritten in the wave number representation as

$$\begin{aligned} \partial_t f_{\mathbf{k}} + ik_{\parallel} v_{\parallel} f_{\mathbf{k}} - \frac{c}{B} \sum_{\mathbf{k}'+\mathbf{k}''=\mathbf{k}} [\mathbf{b} \cdot (\mathbf{k}' \times \mathbf{k}'')] \phi_{\mathbf{k}'} f_{\mathbf{k}''} \\ = i \left[\omega_{*i} \left\{ 1 + \eta_i \left(\frac{m_i v_{\parallel}^2}{2T_i} - \frac{1}{2} \right) \right\} - k_{\parallel} v_{\parallel} \right] F_M \frac{e\phi_{\mathbf{k}}}{T_i}, \end{aligned} \quad (4)$$

where $k_{\parallel} \equiv \mathbf{k} \cdot \mathbf{b}$ is the parallel wave number and the parallel nonlinearity $(e/m_i)E_{\parallel} \partial \tilde{f} / \partial v_{\parallel}$ in Eq. (1) is neglected. In Eq. (4), inhomogeneities in the background density and temperature are taken into account only through $\omega_{*i} \equiv (cT_i/eB)\mathbf{k}_{\perp} \cdot \mathbf{b} \times \nabla \ln n_0$ and $\eta_i \equiv d \ln T_i / d \ln n_0$ while n_0 and T_i in other places as well as ω_{*i} and η_i are regarded as constants. Taking the velocity moments of Eq. (4), we obtain fluid equations

$$\begin{aligned} \partial_t n_{\mathbf{k}} + ik_{\parallel} n_0 u_{\mathbf{k}} - i\omega_{*i} n_0 \frac{e\phi_{\mathbf{k}}}{T_i} \\ - \frac{c}{B} \sum_{\mathbf{k}'+\mathbf{k}''=\mathbf{k}} [\mathbf{b} \cdot (\mathbf{k}' \times \mathbf{k}'')] \phi_{\mathbf{k}'} n_{\mathbf{k}''} = 0, \end{aligned} \quad (5)$$

$$\begin{aligned} n_0 m_i \partial_t u_{\mathbf{k}} + ik_{\parallel} (T_i n_{\mathbf{k}} + n_0 T_{\mathbf{k}} + n_0 e \phi_{\mathbf{k}}) \\ - \frac{n_0 m_i c}{B} \sum_{\mathbf{k}'+\mathbf{k}''=\mathbf{k}} [\mathbf{b} \cdot (\mathbf{k}' \times \mathbf{k}'')] \phi_{\mathbf{k}'} u_{\mathbf{k}''} = 0, \end{aligned} \quad (6)$$

$$\begin{aligned} n_0 \partial_t T_{\mathbf{k}} + ik_{\parallel} (2n_0 T_i u_{\mathbf{k}} + q_{\mathbf{k}}) - i\omega_{*i} \eta_i n_0 e \phi_{\mathbf{k}} \\ - \frac{n_0 c}{B} \sum_{\mathbf{k}'+\mathbf{k}''=\mathbf{k}} [\mathbf{b} \cdot (\mathbf{k}' \times \mathbf{k}'')] \phi_{\mathbf{k}'} T_{\mathbf{k}''} = 0, \end{aligned} \quad (7)$$

where $n_{\mathbf{k}}(t) \equiv \int_{-\infty}^{\infty} dv_{\parallel} f_{\mathbf{k}}$, $n_0 u_{\mathbf{k}}(t) \equiv \int_{-\infty}^{\infty} dv_{\parallel} v_{\parallel} f_{\mathbf{k}}$, $n_0 T_{\mathbf{k}}(t) \equiv \int_{-\infty}^{\infty} dv_{\parallel} v_{\parallel}^2 f_{\mathbf{k}}(m_i v_{\parallel}^2 - T_i)$, and $q_{\mathbf{k}}(t) \equiv \int_{-\infty}^{\infty} dv_{\parallel} v_{\parallel}^3 f_{\mathbf{k}}(m_i v_{\parallel}^3 - 3T_i v_{\parallel})$. Here all nonlinear terms result from the $\mathbf{E} \times \mathbf{B}$ drift. From Eq. (2), we also have

$$n_{\mathbf{k}} = n_0 \frac{e\phi_{\mathbf{k}}}{T_e}, \quad (8)$$

which makes the nonlinear terms in Eq. (5) vanish. A system of the fluid equations (5)–(7) and the quasineutrality condi-

tion (8) are not closed because the parallel heat flow $q_{\mathbf{k}}$ is included in Eq. (7). A new collisionless closure model for $q_{\mathbf{k}}$ is given in Sec. II C. Before presenting the closure model, it is useful to review the linear kinetic solution of Eqs. (4) and (8) in the next subsection.

B. Linear kinetic solution

Here, we consider the linear solution of Eqs. (4) and (8) for a specified wave number vector \mathbf{k} . The initial-value problem of the linearized version of Eqs. (4) and (8) is easily solved by using the Laplace transform. The linear solutions $f_{\mathbf{k}}(v_{\parallel}, t)$ and $\phi_{\mathbf{k}}(t)$ are written by

$$[f_{\mathbf{k}}(v_{\parallel}, t), \phi_{\mathbf{k}}(t)] = \int_C \frac{d\omega}{2\pi} [f_{\mathbf{k}}(v_{\parallel}, \omega), \phi_{\mathbf{k}}(\omega)] e^{-i\omega t}, \tag{9}$$

where C is a contour in the complex ω -plane which lies above all of the singular points of the integrand. Here, $f_{\mathbf{k}}(v_{\parallel}, \omega)$ and $\phi_{\mathbf{k}}(\omega)$ are given by

$$f_{\mathbf{k}}(v_{\parallel}, \omega) = \left[-1 + \frac{\omega - \omega_{*i} \{1 + \eta_i(m_i v_{\parallel}^2 / 2T_i - 1/2)\}}{\omega - k_{\parallel} v_{\parallel}} \right] F_M \times \frac{e \phi_{\mathbf{k}}(\omega)}{T_i} + \frac{if_{\mathbf{k}}(v_{\parallel}, t=0)}{\omega - k_{\parallel} v_{\parallel}} \tag{10}$$

and

$$\frac{e \phi_{\mathbf{k}}(\omega)}{T_i} = \frac{I_{\mathbf{k}}(\omega)}{D_{\mathbf{k}}(\omega)}, \tag{11}$$

respectively, where the dispersion function $D_{\mathbf{k}}(\omega)$ is defined by

$$D_{\mathbf{k}}(\omega) \equiv 1 + \frac{T_i}{T_e} - \frac{1}{n_0} \int_L dv_{\parallel} F_M \times \frac{\omega - \omega_{*i} \{1 + \eta_i(m_i v_{\parallel}^2 / 2T_i - 1/2)\}}{\omega - k_{\parallel} v_{\parallel}} \tag{12}$$

and

$$I_{\mathbf{k}}(\omega) \equiv \frac{1}{n_0} \int_L dv_{\parallel} \frac{if(v_{\parallel}, t=0)}{\omega - k_{\parallel} v_{\parallel}}. \tag{13}$$

In Eqs. (12) and (13), L is a Landau contour in the complex v_{\parallel} -plane which pass below the singular point $v_{\parallel} = \omega/k_{\parallel}$ for $k_{\parallel} > 0$ (above the singular point for $k_{\parallel} < 0$).

We consider the *normal-mode* solution which takes the form of

$$[f_{\mathbf{k}}^{(nm)}(v_{\parallel}, t), \phi_{\mathbf{k}}^{(nm)}(t)] \equiv [f_{L\mathbf{k}}(v_{\parallel}), \phi_{L\mathbf{k}}] \exp(-i\omega_{L\mathbf{k}} t). \tag{14}$$

Here, $\phi_{L\mathbf{k}}$ is a constant (the normalization $e \phi_{L\mathbf{k}}/T_i = 1$ is used later), $\omega_{L\mathbf{k}}$ is determined by the dispersion relation $D_{\mathbf{k}}(\omega_{L\mathbf{k}}) = 0$, and $f_{L\mathbf{k}}(v_{\parallel})$ is given in terms of $\phi_{L\mathbf{k}}$ as

$$f_{L\mathbf{k}}(v_{\parallel}) = \left[-1 + \frac{\omega_{L\mathbf{k}} - \omega_{*i} \{1 + \eta_i(m_i v_{\parallel}^2 / 2T_i - 1/2)\}}{\omega_{L\mathbf{k}} - k_{\parallel} v_{\parallel}} \right] F_M \times \frac{e \phi_{L\mathbf{k}}}{T_i}. \tag{15}$$

Here, the system is assumed to be linearly unstable and the most unstable mode which has the largest growth rate $\text{Im}(\omega_{L\mathbf{k}}) (> 0)$ is considered. We can directly confirm that the normal-mode solution in Eq. (14) satisfies the linearized version of Eqs. (4) and (8). Also, as well known, asymptotic behaviors of general linear solutions are dominantly described by the normal-mode solution which has the largest growth rate.

When we use the Fourier transform in time instead of the Laplace transform, we find that $D_{0\mathbf{k}}(\omega_{L\mathbf{k}}) = 0$ as well as $D_{0\mathbf{k}}(\omega_{L\mathbf{k}}^*) = 0$ are satisfied for the linearly-unstable case $\text{Im}(\omega_{L\mathbf{k}}) > 0$, where $\omega_{L\mathbf{k}}^*$ denotes the complex conjugate of $\omega_{L\mathbf{k}}$ and $D_{0\mathbf{k}}$ is defined by Eq. (12) with the real v_{\parallel} -axis used instead of the Landau contour L . Corresponding to this complex conjugate $\omega_{L\mathbf{k}}^*$, let us take the complex conjugate of the normal-mode solution

$$[f_{\mathbf{k}}^{(cc)}(v_{\parallel}, t), \phi_{\mathbf{k}}^{(cc)}(t)] \equiv [f_{L\mathbf{k}}^*(v_{\parallel}), \phi_{L\mathbf{k}}^*] \exp(-i\omega_{L\mathbf{k}}^* t). \tag{16}$$

Substituting Eq. (16) into Eq. (13) and using Eqs. (9)–(15), $e \phi_{L\mathbf{k}}/T_i = 1$ and $D_{\mathbf{k}}(\omega_{L\mathbf{k}}) = D_{0\mathbf{k}}(\omega_{L\mathbf{k}}) = 0$, we find that, for the initial condition $f_{\mathbf{k}}(v_{\parallel}, t=0) = f_{L\mathbf{k}}^*(v_{\parallel})$

$$I_{\mathbf{k}}(\omega) = \frac{iD_{\mathbf{k}}(\omega)}{\omega - \omega_{L\mathbf{k}}^*}, \quad \frac{e \phi_{\mathbf{k}}(\omega)}{T_i} = \frac{i}{\omega - \omega_{L\mathbf{k}}^*},$$

$$f_{\mathbf{k}}(v_{\parallel}, \omega) = \frac{if_{L\mathbf{k}}^*(v_{\parallel})}{\omega - \omega_{L\mathbf{k}}^*}, \quad \frac{e \phi_{\mathbf{k}}(t)}{T_i} = \exp(-i\omega_{L\mathbf{k}}^* t), \tag{17}$$

$$f_{\mathbf{k}}(v_{\parallel}, t) = f_{L\mathbf{k}}^*(v_{\parallel}) \exp(-i\omega_{L\mathbf{k}}^* t),$$

which show that *the complex conjugate of the normal-mode solution in Eq. (16) is a linear solution of Eqs. (4) and (8) as well as the normal-mode solution*. Since $\text{Im}(\omega_{L\mathbf{k}}) > 0$ is assumed, the complex-conjugate solution exponentially damps in the course of time. The existence of the complex-conjugate solution is related to the *time reversal symmetry* of the original kinetic equation and it should not be confused with what results from the reality condition in the Fourier representation. We should note that, for the case of $\text{Im}(\omega_{L\mathbf{k}}) < 0$, the complex-conjugate of the normal-mode solution is *not* a linear solution of Eqs. (4) and (8) as shown from $D_{\mathbf{k}}(\omega_{L\mathbf{k}}) \neq D_{0\mathbf{k}}(\omega_{L\mathbf{k}})$.

C. Closure model

Let us consider a closure problem for the parallel heat flow term $q_{\mathbf{k}}$ in Eq. (7). Using Eqs. (8) and (9) in Ref. 15 to give $q_{\mathbf{k}}^{(nm)}$ and $T_{\mathbf{k}}^{(nm)}$, respectively, with the phase velocity $\mathcal{W} \rightarrow \omega_{L\mathbf{k}}/k_{\parallel}$, we find that, for the normal-mode solution given in the previous subsection, the parallel heat flow is related to the temperature perturbation as

$$q_{\mathbf{k}}^{(nm)}(t) = C_{L\mathbf{k}} n_0 v_i T_{\mathbf{k}}^{(nm)}(t), \tag{18}$$

where $v_{ii} \equiv \sqrt{T_i/m_i}$, $n_0 T_{\mathbf{k}}^{(nm)}(t) \equiv \int dv_{\parallel} f_{\mathbf{k}}^{(nm)}(v_{\parallel}, t) (m_i v_{\parallel}^2 - T_i)$, and $q_{\mathbf{k}}^{(nm)}(t) \equiv \int dv_{\parallel} f_{\mathbf{k}}^{(nm)}(v_{\parallel}, t) (m_i v_{\parallel}^3 - 3T_i v_{\parallel})$. The coefficient $C_{L\mathbf{k}}$ is defined by

$$C_{L\mathbf{k}} = B \left(\frac{\omega_{L\mathbf{k}}}{k_{\parallel} v_i} \right), \tag{19}$$

where $B(w)$ is defined by¹⁵

$$B(w) \equiv -\frac{1}{\sqrt{2}} \frac{Z^{(3)}(w/\sqrt{2})}{Z^{(2)}(w/\sqrt{2})} \quad (20)$$

for $k_{\parallel} > 0$. Here, $Z^{(n)}(\zeta)$ denotes the n th derivative of the plasma dispersion function $Z(\zeta)$ defined by

$$Z(\zeta) = \frac{1}{\sqrt{\pi}} \int_{-\infty}^{+\infty} \frac{e^{-\beta^2}}{\beta - \zeta} d\beta \quad (21)$$

for $\text{Im}(\zeta) > 0$ and by its analytic continuation for $\text{Im}(\zeta) < 0$. For $k_{\parallel} < 0$, $B(w)$ is determined by the relation $B_+(w) = [B_-(w^*)]^*$ where $B_+(w)$ and $B_-(w)$ denote $B(w)$ for $k_{\parallel} > 0$ and $B(w)$ for $k_{\parallel} < 0$, respectively, and $*$ represents the complex conjugate.

The closure relation given by Eqs. (18)–(21), which is exactly valid for the linear normal-mode solution, is the one which is well reproduced by conventional linear kinetic-fluid closure models by Hammitt and Perkins,¹⁰ and by Chang and Callen.¹¹ In the limit of $\omega_{Lk}/k_{\parallel}v_t \rightarrow 0$, we obtain $C_{Lk} = -2(2/\pi)^{1/2}ik_{\parallel}/|k_{\parallel}|$. This case corresponds to the result by Hammitt and Perkins (hp), in which Eq. (18) leads to the *dissipative* parallel heat flow $q_{\mathbf{k}} = -n_0\chi_{\parallel}^{\text{hp}}ik_{\parallel}T_{\mathbf{k}}$ with the parallel heat diffusivity $\chi_{\parallel}^{\text{hp}} = 2(2/\pi)^{1/2}v_t/|k_{\parallel}|$. Chang and Callen suggested in Eqs. (54)–(61) of Ref. 11 that simplified versions of normal-mode closure relations, which are obtained by replacing ω_{Lk} with $i\partial_t$ under the conditions such as the adiabatic region and the one-pole approximation, should be used for numerical simulations. These conventional linear closure models cause the *dissipation or time irreversibility* for both stable and unstable modes. Hammitt and Perkins¹⁰ showed that there exists a non-Maxwellian equilibrium function $f_0(v_{\parallel})$ for which their closure gives an exact linear response to the electrostatic potential and accordingly an exact dispersion relation for the normal mode. However, this does not imply that their closure exactly describes any linear solution of the initial value problem with an arbitrary initial perturbation $f_{\mathbf{k}}(v_{\parallel}, t=0)$ added to that equilibrium. For example, the complex-valued frequency ω_{Lk}^* of the complex-conjugate solution derives not from the dispersion function $D_{\mathbf{k}}(\omega)$ but from the initial condition term $I_{\mathbf{k}}(\omega)$ [see Eq. (17)]. In this case of the complex-conjugate solution, their closure cannot correctly give the parallel heat flow $q_{\mathbf{k}}$ as shown below.

It is easily found that, for the complex-conjugate solution in Eq. (16), the parallel heat flow is related to the temperature perturbation in terms of C_{Lk}^* (complex conjugate of C_{Lk}) as

$$q_{\mathbf{k}}^{(cc)}(t) = C_{Lk}^* n_0 v_t T_{\mathbf{k}}^{(cc)}(t), \quad (22)$$

where $n_0 T_{\mathbf{k}}^{(cc)}(t) \equiv \int dv_{\parallel} f_{\mathbf{k}}^{(cc)}(v_{\parallel}, t)(m_i v_{\parallel}^2 - T_i)$ and $q_{\mathbf{k}}^{(cc)}(t) \equiv \int dv_{\parallel} f_{\mathbf{k}}^{(cc)}(v_{\parallel}, t)(m_i v_{\parallel}^3 - 3T_i v_{\parallel})$. For the complex-conjugate solution, the phase difference between $q_{\mathbf{k}}$ and $T_{\mathbf{k}}$, which is an important element to consider by closure models, is opposite to that for the normal mode as seen from Eqs. (18) and (22). We should note that the conventional linear closure models can not describe the relation in Eq. (22) for the complex-conjugate solution and that this is the reason why they fail to reproduce the amplitude oscillations of the

nonlinear solution of the three-mode ITG problem as shown in Sec. III. In order to keep the time reversal symmetry of the original kinetic equation, closure models need to be valid for both cases of the normal-mode solution and the complex-conjugate solution. In our new collisionless fluid closure model, the parallel heat flux is related to the lower-order moments (i.e., density, parallel flow, and temperature perturbations) such that *this relation is valid both for the normal-mode solution and the complex-conjugate solution as well as for any linear combination of these solutions*. Let us express such a closure relation by $q_{\mathbf{k}} = F_{\mathbf{k}}(T_{\mathbf{k}}, u_{\mathbf{k}}, n_{\mathbf{k}})$. For distribution functions given by linear combinations of the normal-mode solution and the complex-conjugate solution $f_{\mathbf{k}} = \alpha_{\mathbf{k}}^> f_{\mathbf{k}}^{(nm)} + \alpha_{\mathbf{k}}^< f_{\mathbf{k}}^{(cc)} = \alpha_{\mathbf{k}}^> f_{Lk} e^{-i\omega_{Lk}t} + \alpha_{\mathbf{k}}^< f_{Lk}^* e^{-i\omega_{Lk}^*t}$, the density, parallel flow, temperature, and parallel heat flow are written as

$$\begin{aligned} n_{\mathbf{k}} &= \alpha_{\mathbf{k}}^> n_{\mathbf{k}}^{(nm)} + \alpha_{\mathbf{k}}^< n_{\mathbf{k}}^{(cc)} \\ &= \alpha_{\mathbf{k}}^> n_{Lk} e^{-i\omega_{Lk}t} + \alpha_{\mathbf{k}}^< n_{Lk}^* e^{-i\omega_{Lk}^*t}, \\ u_{\mathbf{k}} &= \alpha_{\mathbf{k}}^> u_{\mathbf{k}}^{(nm)} + \alpha_{\mathbf{k}}^< u_{\mathbf{k}}^{(cc)} \\ &= \alpha_{\mathbf{k}}^> u_{Lk} e^{-i\omega_{Lk}t} + \alpha_{\mathbf{k}}^< u_{Lk}^* e^{-i\omega_{Lk}^*t}, \\ T_{\mathbf{k}} &= \alpha_{\mathbf{k}}^> T_{\mathbf{k}}^{(nm)} + \alpha_{\mathbf{k}}^< T_{\mathbf{k}}^{(cc)} \\ &= \alpha_{\mathbf{k}}^> T_{Lk} e^{-i\omega_{Lk}t} + \alpha_{\mathbf{k}}^< T_{Lk}^* e^{-i\omega_{Lk}^*t}, \\ q_{\mathbf{k}} &= \alpha_{\mathbf{k}}^> q_{\mathbf{k}}^{(nm)} + \alpha_{\mathbf{k}}^< q_{\mathbf{k}}^{(cc)} \\ &= \alpha_{\mathbf{k}}^> q_{Lk} e^{-i\omega_{Lk}t} + \alpha_{\mathbf{k}}^< q_{Lk}^* e^{-i\omega_{Lk}^*t}, \end{aligned} \quad (23)$$

where $\alpha_{\mathbf{k}}^>$ and $\alpha_{\mathbf{k}}^<$ are arbitrary constants. Substituting these expressions into the closure relation, we obtain

$$\begin{aligned} F_{\mathbf{k}}(\alpha_{\mathbf{k}}^> T_{\mathbf{k}}^{(nm)} + \alpha_{\mathbf{k}}^< T_{\mathbf{k}}^{(cc)}, \alpha_{\mathbf{k}}^> u_{\mathbf{k}}^{(nm)} + \alpha_{\mathbf{k}}^< u_{\mathbf{k}}^{(cc)}, \\ \alpha_{\mathbf{k}}^> n_{\mathbf{k}}^{(nm)} + \alpha_{\mathbf{k}}^< n_{\mathbf{k}}^{(cc)}) &= \alpha_{\mathbf{k}}^> F_{\mathbf{k}}(T_{\mathbf{k}}^{(nm)}, u_{\mathbf{k}}^{(nm)}, n_{\mathbf{k}}^{(nm)}) \\ &\quad + \alpha_{\mathbf{k}}^< F_{\mathbf{k}}(T_{\mathbf{k}}^{(cc)}, u_{\mathbf{k}}^{(cc)}, n_{\mathbf{k}}^{(cc)}). \end{aligned} \quad (24)$$

Therefore, we write the closure relation $q_{\mathbf{k}} = F_{\mathbf{k}}(T_{\mathbf{k}}, u_{\mathbf{k}}, n_{\mathbf{k}})$ in terms of a linear function of $(T_{\mathbf{k}}, u_{\mathbf{k}}, n_{\mathbf{k}})$ as

$$\begin{aligned} q_{\mathbf{k}} &= C_{T\mathbf{k}} n_0 v_t T_{\mathbf{k}} + C_{u\mathbf{k}} n_0 T_i u_{\mathbf{k}} \\ &\quad + C_{n\mathbf{k}} v_t T_i n_{\mathbf{k}} \quad (\text{for linearly unstable modes}). \end{aligned} \quad (25)$$

Furthermore, from comparison between the cases of $(\alpha_{\mathbf{k}}^>, \alpha_{\mathbf{k}}^<) = (1, 0)$ and $(0, 1)$ in Eq. (24), we find that $F_{\mathbf{k}}(T_{Lk}^*, u_{Lk}^*, n_{Lk}^*) = [F_{\mathbf{k}}(T_{Lk}, u_{Lk}, n_{Lk})]^*$ and, therefore, the dimensionless coefficients $C_{T\mathbf{k}}$, $C_{u\mathbf{k}}$, and $C_{n\mathbf{k}}$ in Eq. (25) are *real-valued* constants determined so as to satisfy

$$C_{T\mathbf{k}} n_0 v_t T_{Lk} + C_{u\mathbf{k}} n_0 T_i u_{Lk} + C_{n\mathbf{k}} v_t T_i n_{Lk} = C_{Lk} n_0 v_t T_{Lk}. \quad (26)$$

Equation (26) is required from Eqs. (18) and (25). Equation (25) is called the nondissipative closure model (NCM) hereafter. Here, C_{Lk} is given by Eq. (19), and

$$\begin{aligned} \frac{n_{Lk}}{n_0} &\equiv \frac{1}{n_0} \int dv_{\parallel} f_{Lk}(v_{\parallel}) = \frac{e \phi_{Lk}}{T_e}, \\ u_{Lk} &\equiv \frac{1}{n_0} \int dv_{\parallel} f_{Lk}(v_{\parallel}) v_{\parallel} = \frac{e \phi_{Lk}}{T_e} \frac{(\omega_{Lk} - \omega_{*e})}{k_{\parallel}}, \\ T_{Lk} &\equiv \frac{1}{n_0} \int dv_{\parallel} f_{Lk}(v_{\parallel}) (m_i v_{\parallel}^2 - T_i) \\ &= \frac{e \phi_{Lk}}{T_e} \left[m_i \frac{\omega_{Lk}(\omega_{Lk} - \omega_{*e})}{k_{\parallel}^2} - T_i - T_e \right], \end{aligned} \quad (27)$$

where $\omega_{*e} \equiv -(T_e/T_i)\omega_{*i}$. We obtain from Eqs. (26) and (27)

$$\begin{aligned} C_{Tk} &= C_{Lrk} - C_{Lik} \frac{\text{Re}(\xi_k \zeta_k^*)}{\text{Im}(\xi_k \zeta_k^*)} - C_{nk} \frac{\xi_{ik}}{\text{Im}(\xi_k \zeta_k^*)}, \\ C_{uk} &= C_{Lik} \frac{|\zeta_k|^2}{\text{Im}(\xi_k \zeta_k^*)} + C_{nk} \frac{\xi_{ik}}{\text{Im}(\xi_k \zeta_k^*)}, \end{aligned} \quad (28)$$

where $C_{Lk} \equiv C_{Lrk} + iC_{Lik}$, $\xi_k \equiv \xi_{rk} + i\xi_{ik} \equiv (\omega_{Lk} - \omega_{*e})/(k_{\parallel}v_i)$, and $\zeta_k \equiv \zeta_{rk} + i\zeta_{ik} \equiv \omega_{Lk}(\omega_{Lk} - \omega_{*e})/(k_{\parallel}^2v_i^2) - 1 - T_e/T_i$ are used. For arbitrarily given C_{nk} , the closure relation in Eq. (25) with Eq. (28) satisfies the requirement described before Eq. (23). In order to uniquely determine (C_{Tk}, C_{uk}, C_{nk}) , we impose an additional condition that Eq. (25) should be valid when the perturbation distribution function takes a Maxwellian form, $f_k \propto \exp(-m_i v^2/2T_i)$, for which $u_k = T_k = q_k = 0$. Then, we obtain

$$C_{nk} = 0, \quad (29)$$

from which with Eq. (28), C_{Tk} and C_{uk} are also uniquely determined.

So far, we have considered only linearly unstable modes [$\text{Im}(\omega_{Lk}) > 0$]. As mentioned at the end of Sec. II B, the complex-conjugate of the normal mode is not a linear solution for $\text{Im}(\omega_{Lk}) < 0$. Thus, for linearly stable modes, we assume the normal mode to be a dominant contribution to the perturbation, and use the same closure relation as in Eq. (18)

$$q_k = C_{Lk} n_0 v_i T_k \quad (\text{for linearly stable modes}), \quad (30)$$

where C_{Lk} is defined by Eq. (19). It may appear that different closure relations for unstable and stable modes give discontinuity in the parallel heat flux q_k across the point of marginal stability [$\text{Im}(\omega_{Lk}) = 0$]. However, as seen from Eq. (26), we find that, even if apparent forms are different, the NCM in Eq. (25) give the same q_k as Eq. (30) when the fluid variables (T_k, u_k, n_k) are described by the unstable normal mode, (T_{Lk}, u_{Lk}, n_{Lk}) . Thus, the discontinuity in q_k across the marginal point does not occur if the fluid variables change continuously and are dominated by the normal mode near the marginal point.

D. Entropy balances

It is useful to consider entropy balances in nonequilibrium systems for understanding the relation between entropy production, dissipation, thermodynamic forces, and transport fluxes. Here, kinetic and fluid entropy balances are examined for the turbulent system governed by the equations in Sec.

II A in order to elucidate the role of the closure model for the turbulence saturation and the anomalous transport.

We define the microscopic entropy S_m and macroscopic entropy S_M for ions per unit volume by²⁰

$$S_m = - \int dv_{\parallel} f \ln f, \quad (31)$$

$$S_M = - \int dv_{\parallel} F_M \ln F_M, \quad (32)$$

where $f = F_M + \tilde{f}$. Retaining terms up to $\mathcal{O}(\tilde{f}^2)$, the relation between S_m and S_M is given by

$$S_M = \langle S_m \rangle + \frac{1}{2} \int dv_{\parallel} \frac{\langle \tilde{f}^2 \rangle}{F_M}, \quad (33)$$

where $\langle \dots \rangle$ represents the ensemble average. As shown from the basic kinetic equation (1) [or Eq. (4)], the total microscopic entropy $\int d^3x S_m$ is conserved without collisions, although the macroscopic entropy S_M or $\Delta S \equiv \frac{1}{2} \int dv_{\parallel} \langle \tilde{f}^2 \rangle / F_M$ can be produced by the turbulent or anomalous transport process. Krommes and Hu¹⁹ called $\bar{S} \equiv -\frac{1}{2} \int dv_{\parallel} \langle \tilde{f}^2 \rangle / F_M$ ($= S_m - S_M$ in our notation) the entropy of the system to measure deviation of the fluctuating distribution function \tilde{f} from the ensemble-averaged distribution function $\langle f \rangle$. Here, we regard $\Delta S = S_M - S_m$ ($= -\bar{S} = \bar{\mathcal{F}}$ in Krommes and Hu¹⁹) as the entropy associated with the fluctuations because, in the collisionless system, turbulent processes produce not S_m but S_M . From Eq. (4), we find that the turbulent entropy production rate is given by

$$\begin{aligned} \frac{d}{dt} \left(\sum_{\mathbf{k}} \int dv_{\parallel} \frac{|f_{\mathbf{k}}|^2}{2F_M} \right) &= n_0 \sum_{\mathbf{k}} \left[\text{Re} \left(\frac{T_{\mathbf{k}}}{2T_i} \mathbf{v}_{E\mathbf{k}}^* \right) \cdot (-\nabla \ln T_i) \right. \\ &\quad \left. + \frac{e \text{Re}(E_{\parallel\mathbf{k}} u_{\mathbf{k}}^*)}{T_i} \right] \\ &= \frac{\mathbf{q}_{\perp}}{T_i} \cdot (-\nabla \ln T_i) + \frac{Q}{T_i}, \end{aligned} \quad (34)$$

where $\mathbf{v}_{E\mathbf{k}} \equiv i(c/B)\mathbf{b} \times \mathbf{k} \phi_{\mathbf{k}}$ is the turbulent $\mathbf{E} \times \mathbf{B}$ velocity, $\mathbf{q}_{\perp} \equiv \frac{1}{2} n_0 \sum_{\mathbf{k}} \text{Re}(T_{\mathbf{k}} \mathbf{v}_{E\mathbf{k}}^*)$ is the turbulent perpendicular heat flux, $E_{\parallel\mathbf{k}} \equiv -ik_{\parallel} \phi_{\mathbf{k}}$ is the parallel electric field, and $Q \equiv en_0 \sum_{\mathbf{k}} \text{Re}(E_{\parallel\mathbf{k}} u_{\mathbf{k}}^*)$ represents the turbulent ion heating.

Using Eqs. (5) and (8), we obtain

$$\frac{d}{dt} \left(\sum_{\mathbf{k}} \frac{n_0}{2} \left| \frac{e \phi_{\mathbf{k}}}{T_e} \right|^2 \right) = - \frac{Q}{T_e}. \quad (35)$$

Then, using Eqs. (35), the kinetic entropy balance equation (34) is rewritten as

$$\frac{d}{dt} \sum_{\mathbf{k}} \left(\int dv_{\parallel} \frac{|f_{\mathbf{k}}|^2}{2F_M} + \frac{n_0 T_e}{2T_i} \left| \frac{e \phi_{\mathbf{k}}}{T_e} \right|^2 \right) = \frac{\mathbf{q}_{\perp}}{T_i} \cdot (-\nabla \ln T_i). \quad (36)$$

It is convenient to expand $f_{\mathbf{k}}$ in terms of the Hermite polynomials $H_n(x) \equiv (-1)^n e^{x^2/2} d^n e^{-x^2/2} / dx^n$ ($x \equiv v_{\parallel}/v_i; n = 0, 1, 2, \dots$) as

$$\begin{aligned}
 f_{\mathbf{k}}(v_{\parallel}, t) &= F_M(v_{\parallel}) \sum_n \varphi_{n\mathbf{k}}(t) H_n(v_{\parallel}/v_t) \\
 &= F_M(v_{\parallel}) \left[\frac{n_{\mathbf{k}}}{n_0} + \frac{u_{\mathbf{k}}}{v_t} \left(\frac{v_{\parallel}}{v_t} \right) + \frac{1}{2} \frac{T_{\mathbf{k}}}{T_i} \left(\left(\frac{v_{\parallel}}{v_t} \right)^2 - 1 \right) \right. \\
 &\quad \left. + \frac{1}{6} \frac{q_{\mathbf{k}}}{n_0 T_i v_t} \left(\left(\frac{v_{\parallel}}{v_t} \right)^3 - 3 \left(\frac{v_{\parallel}}{v_t} \right) \right) \right. \\
 &\quad \left. + \sum_{n \geq 4} \varphi_{n\mathbf{k}}(t) H_n(v_{\parallel}/v_t) \right], \tag{37}
 \end{aligned}$$

where $\varphi_{n\mathbf{k}}(t) = (n!)^{-1} \int_{-\infty}^{\infty} d(v_{\parallel}/v_t) f_{\mathbf{k}}(v_{\parallel}, t) H_n(v_{\parallel}/v_t)$ ($n = 0, 1, 2, \dots$). Substituting Eq. (37) into Eq. (36) gives

$$\begin{aligned}
 \frac{d}{dt} \sum_{\mathbf{k}} n_0 \left(\frac{1}{2} \left| \frac{n_{\mathbf{k}}}{n_0} \right|^2 + \frac{1}{2} \left| \frac{u_{\mathbf{k}}}{v_t} \right|^2 + \frac{1}{4} \left| \frac{T_{\mathbf{k}}}{T_i} \right|^2 + \frac{1}{12} \left| \frac{q_{\mathbf{k}}}{n_0 T_i v_t} \right|^2 \right. \\
 \left. + \sum_{n \geq 4} \frac{n!}{2} |\varphi_{n\mathbf{k}}|^2 + \frac{T_e}{2T_i} \left| \frac{e\phi_{\mathbf{k}}}{T_e} \right|^2 \right) = \frac{\mathbf{q}_{\perp}}{T_i} \cdot (-\nabla \ln T_i), \tag{38}
 \end{aligned}$$

where the orthogonality conditions for the Hermite polynomials $(2\pi)^{-1/2} \int_{-\infty}^{\infty} dx e^{-x^2/2} H_n(x) H_m(x) = n! \delta_{nm}$ ($n, m = 0, 1, 2, \dots$) are used. It is found from Eq. (36) or Eq. (38) that there is no perpendicular heat transport in the direction of the temperature gradient in the collisionless and steady turbulent state where saturation of the entropy $\int dv_{\parallel} |f_{\mathbf{k}}|^2 / 2F_M$ and the potential amplitude $|\phi_{\mathbf{k}}|$ occurs. [If the collision term and the parallel-nonlinearity term are retained in Eq. (4), there appear corresponding terms which balance the heat transport term in the right-hand side of Eqs. (36) and (38), although they are typically small.^{2]} Then, in order to treat the anomalous transport in the collisionless turbulent plasma, we assume a *quasisteady* state in which the amplitudes of the fluid variables $\varphi_{n\mathbf{k}}$ with low n ($n_{\mathbf{k}}, u_{\mathbf{k}}, T_{\mathbf{k}}, q_{\mathbf{k}}, \dots$) and the potential $\phi_{\mathbf{k}}$ reach the steady state while the high- n moments included in $\sum_{n \geq 4} (n!/2) |\varphi_{n\mathbf{k}}|^2$ grow indefinitely in time. The quasisteady state should be regarded as idealization of the real steady state in which those high- n moments eventually saturate as well due to collisional dissipation even if the collision frequency is much smaller than the characteristic frequency of the instabilities causing the turbulence. We should note that the moments with higher n are more effectively dissipated by the Fokker–Planck-type collision operator because they represents finer structure with steep gradients in the velocity space.

Using Eqs. (5)–(8), we can derive another balance equation similar to Eq. (38)

$$\begin{aligned}
 \frac{d}{dt} \sum_{\mathbf{k}} n_0 \left(\frac{1}{2} \left| \frac{n_{\mathbf{k}}}{n_0} \right|^2 + \frac{1}{2} \left| \frac{u_{\mathbf{k}}}{v_t} \right|^2 + \frac{1}{4} \left| \frac{T_{\mathbf{k}}}{T_i} \right|^2 + \frac{T_e}{2T_i} \left| \frac{e\phi_{\mathbf{k}}}{T_e} \right|^2 \right) \\
 = \frac{\mathbf{q}_{\perp}}{T_i} \cdot (-\nabla \ln T_i) + \sum_{\mathbf{k}} \operatorname{Re} \left(\frac{T_{\mathbf{k}}}{2T_i^2} i k_{\parallel} q_{\mathbf{k}}^* \right), \tag{39}
 \end{aligned}$$

which can be regarded as the fluid entropy balance equation. Comparing Eq. (39) to Eq. (38), we easily find

$$\begin{aligned}
 \sum_{\mathbf{k}} \operatorname{Re} \left(\frac{T_{\mathbf{k}}}{2T_i^2} i k_{\parallel} q_{\mathbf{k}}^* \right) = -\frac{d}{dt} \sum_{\mathbf{k}} n_0 \left(\frac{1}{12} \left| \frac{q_{\mathbf{k}}}{n_0 T_i v_t} \right|^2 \right. \\
 \left. + \sum_{n \geq 4} \frac{n!}{2} |\varphi_{n\mathbf{k}}|^2 \right). \tag{40}
 \end{aligned}$$

For the quasisteady state in which $d(\sum_{n \leq 3} (n!/2) |\varphi_{n\mathbf{k}}|^2) / dt = 0$, we obtain from Eqs. (39) and (40),

$$\begin{aligned}
 \frac{\mathbf{q}_{\perp}}{T_i} \cdot (-\nabla \ln T_i) = -\sum_{\mathbf{k}} \operatorname{Re} \left(\frac{T_{\mathbf{k}}}{2T_i^2} i k_{\parallel} q_{\mathbf{k}}^* \right) \\
 = \frac{d}{dt} \left(n_0 \sum_{\mathbf{k}} \sum_{n \geq 4} \frac{n!}{2} |\varphi_{n\mathbf{k}}|^2 \right). \tag{41}
 \end{aligned}$$

Equation (41) represents the entropy production rate in the quasisteady state, where the perpendicular heat transport in the presence of the background temperature gradient drives the growth of the fluctuations in the high- n moment variables through the correlation between the parallel heat flux and temperature fluctuations. Thus, it is considered that the entropy production rate and the anomalous perpendicular heat transport are deeply dependent on what closure model is used for the parallel heat flux. If we use the Hammett–Perkins model $q_{\mathbf{k}} = -n_0 \chi_{\parallel}^{\text{hp}} i k_{\parallel} T_{\mathbf{k}}$ with $\chi_{\parallel}^{\text{hp}} = 2(2/\pi)^{1/2} v_t / |k_{\parallel}|$, the entropy production rate is given by

$$\begin{aligned}
 -\sum_{\mathbf{k}} \operatorname{Re} \left(\frac{T_{\mathbf{k}}}{2T_i^2} i k_{\parallel} q_{\mathbf{k}}^* \right) = n_0 \sum_{\mathbf{k}} \frac{1}{2} \chi_{\parallel}^{\text{hp}2} k_{\parallel}^2 \left| \frac{T_{\mathbf{k}}}{T_i} \right|^2 \\
 \text{(for the Hammett–Perkins model),} \tag{42}
 \end{aligned}$$

which takes the form of the dissipation for all wave number vectors \mathbf{k} . On the other hand, when we use the NCM in Eqs. (25)–(29) and Eq. (30), we obtain

$$\begin{aligned}
 -\operatorname{Re} \left(\frac{T_{\mathbf{k}}}{2T_i^2} i k_{\parallel} q_{\mathbf{k}}^* \right) = -\frac{1}{2} n_0 v_t k_{\parallel} \operatorname{Im}(C_{Lk}) \left| \frac{T_{\mathbf{k}}}{T_i} \right|^2 \\
 \text{(for linearly stable modes)} \tag{43}
 \end{aligned}$$

and

$$\begin{aligned}
 -\operatorname{Re} \left(\frac{T_{\mathbf{k}}}{2T_i^2} i k_{\parallel} q_{\mathbf{k}}^* \right) \\
 = -\frac{1}{2} n_0 C_{u\mathbf{k}} \operatorname{Re} \left(\frac{T_{\mathbf{k}}}{T_i} i k_{\parallel} u_{\mathbf{k}}^* \right) \\
 = \frac{1}{4} n_0 C_{u\mathbf{k}} \frac{d}{dt} \left(\left| \frac{n_{\mathbf{k}}}{n_0} \right|^2 + \left| \frac{u_{\mathbf{k}}}{v_t} \right|^2 + \frac{T_e}{T_i} \left| \frac{e\phi_{\mathbf{k}}}{T_e} \right|^2 \right) \\
 - \frac{cn_0 C_{u\mathbf{k}}}{2Bv_t^2} \sum_{\mathbf{k}'+\mathbf{k}''=\mathbf{k}} \operatorname{Re}[\mathbf{b} \cdot (\mathbf{k}' \times \mathbf{k}'') \phi_{\mathbf{k}'} u_{\mathbf{k}''} u_{\mathbf{k}}^*] \\
 \text{(for linearly unstable modes),} \tag{44}
 \end{aligned}$$

where Eqs. (5), (6), and (8) are also used. Then, from Eqs. (43) and (44), the entropy production rate for the quasisteady state is given by

$$\begin{aligned}
 & - \sum_{\mathbf{k}} \operatorname{Re} \left(\frac{T_{\mathbf{k}}}{2T_i^2} ik_{\parallel} q_{\mathbf{k}}^* \right) \\
 & = -n_0 \sum_{\mathbf{k}(\text{stable})} \frac{1}{2} v_t k_{\parallel} \operatorname{Im}(C_{L\mathbf{k}}) \left| \frac{T_{\mathbf{k}}}{T_i} \right|^2 \\
 & \quad - n_0 \sum_{\mathbf{k}(\text{unstable})} \sum_{\mathbf{k}'(\text{stable})} \sum_{\mathbf{k}''=\mathbf{k}-\mathbf{k}''} \frac{cC_{u\mathbf{k}}}{2Bv_t^2} \\
 & \quad \times \operatorname{Re}[\mathbf{b} \cdot (\mathbf{k}' \times \mathbf{k}'') \phi_{\mathbf{k}'} u_{\mathbf{k}''} u_{\mathbf{k}}^*], \tag{45}
 \end{aligned}$$

where $\sum_{\mathbf{k}(\text{stable})}$ ($\sum_{\mathbf{k}(\text{unstable})}$) represents the summation over \mathbf{k} corresponding to linearly stable (linearly unstable) modes. Here, we find that $-v_t k_{\parallel} \operatorname{Im}(C_{L\mathbf{k}}) \sim -v_t k_{\parallel} \lim_{\omega_{L\mathbf{k}}/k_{\parallel} v_t \rightarrow 0} \times \operatorname{Im}(C_{L\mathbf{k}}) = \chi_{\parallel}^{\text{hp}} k_{\parallel}^2 > 0$ and that $C_{u\mathbf{k}} > 0$ for linearly unstable modes. Compared to Eq. (42) for the Hammett–Perkins model, Eq. (45) shows that, in our model, the entropy production rate consists of the dissipation terms for the linearly stable modes [the first group of terms in the right-hand side of Eq. (45)] similar to Eq. (42) and the nondissipative terms (the second group of terms): The latter terms result from the second term in the right-hand side of Eq. (25) and are associated with the transfer of $|u_{\mathbf{k}}^2|$ from the unstable modes to stable modes in the \mathbf{k} -space. Due to this nondissipative nature for unstable modes, turbulence simulations using the NCM may give different results on the entropy production rate and the anomalous heat transport from those obtained by using the conventional closure models. In the next section, an example of application of the NCM is shown.

III. THREE-MODE ITG SYSTEM

Here, we apply the collisionless fluid closure given in the previous section to the three-mode ITG problem.^{2,14}

A. Three-mode ITG equations and exact nonlinear solution

We consider a rectangular domain of $L_x \times L_y$ in the x - y plane with a uniform external magnetic-field $\mathbf{B} = B_0(\hat{\mathbf{z}} + \theta \hat{\mathbf{y}})$ ($|\theta| \ll 1$), where $\hat{\mathbf{y}}$ and $\hat{\mathbf{z}}$ denote the unit vectors in the y and z directions, respectively. The system is assumed to be homogeneous in the z direction ($\partial/\partial z = 0$). The background density and temperature gradients are assumed to exist in the x direction, and their gradient scale lengths are given by $L_n = -(d \ln n_0/dx)^{-1} (> 0)$ and $L_T = -(d \ln T_i/dx)^{-1} (> 0)$, respectively. We employ the periodic boundary conditions in both x and y directions. Then, in Eq. (3), we can write $\mathbf{k} = 2\pi[(m/L_x)\hat{\mathbf{x}} + (n/L_y)\hat{\mathbf{y}}]$, $f_{\mathbf{k}} = f_{m,n}$, and $\phi_{\mathbf{k}} = \phi_{m,n}$ ($m, n = 0, \pm 1, \pm 2, \dots$). In the three-mode ITG system, we only keep $(m, n) = (\pm 1, \pm 1)$ and $(\pm 2, 0)$ modes with the symmetry conditions of $f_{1,1} = f_{-1,1} = f_{1,-1}^* = f_{-1,-1}^*$, $f_{2,0} = f_{-2,0}^*$, and $\operatorname{Re}(f_{2,0}) = 0$. These symmetry conditions imply that the system has boundaries at $x = (2l+1)L_x/4$ ($l = 0, \pm 1, \pm 2, \dots$), where f and ϕ vanish. Here, f_{20} describes a quasi-linear flattening of the temperature profile around $x = 0$, which turns off the linear instability drive for the (1,1) mode. Other modes with higher wave numbers, which may be nonlinearly destabilized by f_{20} steepening the temperature gradient near the boundaries, are not included. Since effects of

finite gyroradii are neglected, we have $\phi_{20} = 0$ and ignore the nonlinear generation of zonal flows, which can play an important role in ITG turbulence.^{5,13,22,23}

Hereafter, $f_{1,1}$, $\operatorname{Im}(f_{2,0})$ and $\phi_{1,1}$ are, respectively, denoted by f_1 , h , and ϕ_1 for simplicity, where f_1 and ϕ_1 are complex-valued while h is real-valued. Then, from Eqs. (4) and (8), the three-mode ITG equations are written as^{2,14}

$$\begin{aligned}
 & (\partial_t + ik\Theta v_{\parallel})f_1(v_{\parallel}, t) + 2ik^2\phi_1(t)h(v_{\parallel}, t) \\
 & = -ik\phi_1(t)G(v_{\parallel}), \tag{46}
 \end{aligned}$$

$$\partial_t h(v_{\parallel}, t) = 4k^2 \operatorname{Im}[\phi_1^*(t)f_1(v_{\parallel}, t)], \tag{47}$$

$$\phi_1(t) = \int dv_{\parallel} f_1(v_{\parallel}, t), \tag{48}$$

where $L_x = L_y = 1/k$ and $T_i = T_e$ (T_e : the electron temperature) are assumed and $G(v_{\parallel})$ is defined by

$$G(v_{\parallel}) \equiv [1 + (v_{\parallel}^2 - 1)\eta_i/2 + \Theta v_{\parallel}]e^{-v_{\parallel}^2/2}/(2\pi)^{-1/2}. \tag{49}$$

Here, we have used dimensionless normalized variables $x = x'/\rho_i$, $y = y'/\rho_i$, $v = v'/v_t$, $t = t'v_t/L_n$, $f = f'L_n v_t/\rho_i n_0$, and $\phi = e\phi'L_n/T_i \rho_i$, where prime represents a dimensional quantity, $v_t = \sqrt{T_i/m_i}$ is the ion thermal velocity, $\rho_i = v_t/\Omega_i$ is the ion thermal gyroradius, and $\Omega_i = eB/m_i c$ is the ion gyrofrequency. Two important parameters Θ and η_i in Eq. (49) are given by $\Theta = \theta L_n/\rho_i$ and $\eta_i = L_n/L_T$, respectively. From Eqs. (46)–(48), the entropy balance equation similar to Eq. (36) is derived as

$$\frac{d}{dt} \left[\int dv_{\parallel} \frac{1}{2F_M} \left(|f_1|^2 + \frac{1}{2}h^2 \right) + \frac{1}{2}|\phi_1|^2 \right] = \eta_i q_x, \tag{50}$$

where $q_x \equiv \operatorname{Re}(\frac{1}{2}T_1 ik\phi_1^*)$ with $T_1 \equiv \int dv_{\parallel} f_1(v_{\parallel}^2 - 1)$ is the heat flux in the x direction, and $F_M \equiv e^{-v_{\parallel}^2/2}/(2\pi)^{1/2}$.

An exact solution of the three-mode ITG equations found by WSS is written as

$$\begin{aligned}
 & f_1(v_{\parallel}, t) = [a(t)f_{Lr}(v_{\parallel}) + ib(t)f_{Li}(v_{\parallel})]\exp(-i\omega_{Lr}t), \\
 & h(v_{\parallel}, t) = c(t)f_{Li}(v_{\parallel}), \tag{51}
 \end{aligned}$$

$$\phi(t) = a(t)\exp(-i\omega_{Lr}t),$$

where $f_{Lr}(v_{\parallel})$ and $f_{Li}(v_{\parallel})$ represent the real and imaginary parts of the eigenfunction $f_L(v_{\parallel}) \equiv f_{L\mathbf{k}}(v_{\parallel})$ in Eq. (15), respectively, and ω_{Lr} is the real part of the eigenfrequency $\omega_{L\mathbf{k}}$ for $\mathbf{k} = (k, k)$. Here, $a(t)$, $b(t)$, and $c(t)$ are real-valued functions of the time t , which satisfy the ordinary differential equations

$$\begin{aligned}
 & da/dt = \gamma b, \\
 & db/dt = \gamma a - 2k^2 ac, \tag{52} \\
 & dc/dt = 4k^2 ab,
 \end{aligned}$$

where $\gamma \equiv \operatorname{Im}(\omega_{L\mathbf{k}})$. These equations are also rewritten in the Hamiltonian form as shown in Appendix A. Functional forms of the solutions $a(t)$, $b(t)$, and $c(t)$ are given in terms of the Jacobi elliptic functions and they are found in Ref. 14. We should note that $a(t)$, $b(t)$, and $c(t)$ are periodic func-

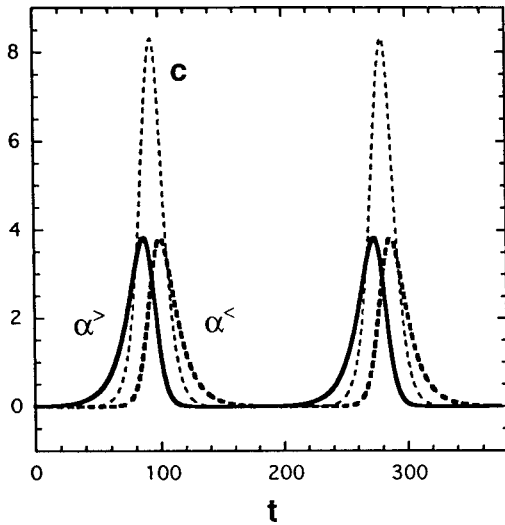


FIG. 1. Amplitudes of the normal mode ($\alpha^>$) and the complex-conjugate mode ($\alpha^<$) as a function of time t for $k=0.1$, $\Theta=1$, $\eta_i=10$, and $\alpha^>(0) = \alpha^<(0) = 0.005$. Also plotted is a curve for $c(t)$.

tions with the period T given by Eq. (32) in Ref. 14 so that the WSS solution in Eq. (51) is *double-periodic* in t with two periods T and $2\pi/\omega_{Lr}$.

Let us define $\alpha^>(t)$ and $\alpha^<(t)$ by

$$\alpha^>(t) = \frac{a(t) + b(t)}{2}, \quad \alpha^<(t) = \frac{a(t) - b(t)}{2}. \quad (53)$$

Then, from Eqs. (51) and (53), we obtain

$$f_1(v_{\parallel}, t) = [\alpha^>(t)f_L(v_{\parallel}) + \alpha^<(t)f_L^*(v_{\parallel})] \exp(-i\omega_{Lr}t), \quad (54)$$

$$\phi(t) = [\alpha^>(t) + \alpha^<(t)] \exp(-i\omega_{Lr}t).$$

Therefore, this exact nonlinear solution is given by the sum of the linear normal-mode solution with the amplitude $\alpha^>(t)$ and the complex conjugate solution with the amplitude $\alpha^<(t)$. The ordinary differential equations (52) are rewritten as

$$d\alpha^>/dt = (\gamma - k^2c)\alpha^> - k^2c\alpha^<, \quad (55)$$

$$d\alpha^</dt = -(\gamma - k^2c)\alpha^< + k^2c\alpha^>, \quad (55)$$

$$dc/dt = 4k^2[(\alpha^>)^2 - (\alpha^<)^2],$$

which show that the normal-mode and complex-conjugate solutions interact with each other through the nonlinear-coupling terms proportional to c . Since the exact nonlinear solution in Eq. (54) is represented as a linear combination of the normal-mode and complex-conjugate solutions, it is accurately described by the the NCM presented in Sec. II C.

Figure 1 shows $\alpha^>(t)$ and $\alpha^<(t)$ obtained from the exact solution for $k=0.1$, $\Theta=1$, $\eta_i=10$, $\alpha^>(0) = \alpha^<(0) = 0.005$ [$a(0)=0.01, b(0)=0$] and $c(0)=0$. For this case, the linear eigenfrequency is given by $\omega_{Lk} = -0.1149 + 0.0831i$ and the period of $[\alpha^>(t), \alpha^<(t), c(t)]$ is $T = 186.78$. We find that peaks of the complex-conjugate-mode amplitude $\alpha^<$ appear after those of the normal-mode amplitude $\alpha^>$. Peaks of the potential amplitude $|\phi(t)| = a(t) = \alpha^>(t) + \alpha^<(t)$ occur between the peaks of $\alpha^<$ and $\alpha^>$ at $t = (n + 1/2)T$ ($n=0, 1, 2, \dots$) where $\alpha^>$ becomes equal

to $\alpha^<$. We should note that, in the nonlinear regimes around the potential's peaks, both the normal mode and its complex conjugate have large amplitudes comparable to each other so that the nonlinear behavior cannot be well described by the conventional linear closure models which do not take account of the complex-conjugate mode. The nonlinear closure model proposed by Mator and Parker succeeded in giving the periodic potential amplitude oscillation in the three-mode ITG problem.¹⁵ Thus, the normal mode and its complex conjugate seem to be included in their model. However, since their nonlinear closure model as well as the local PVT model by Mator¹⁷ assume that the kinetic distribution function $f_{\mathbf{k}}$ is written by a single mode structure corresponding to a dominant complex-valued frequency $\omega_{\mathbf{k}}$, they do not accurately describe the nonlinear states which consist of distinct mode structures with comparable amplitudes as found here. In the next subsection, the closed set of fluid equations for the three-mode ITG system, which are obtained by applying the collisionless fluid closure, are examined in detail.

B. Fluid equations for the three-mode ITG system

Taking the velocity moments of Eqs. (46) and (47), we obtain

$$\partial_t n_1 + ik(\Theta u_1 + \phi_1) = 0, \quad (56)$$

$$\partial_t u_1 + ik\Theta(n_1 + T_1 + \phi_1) + 2ik^2\phi_1 u_h = 0, \quad (57)$$

$$\partial_t u_h - 4k^2 \text{Im}(\phi_1^* u_1) = 0, \quad (58)$$

$$\partial_t T_1 + ik[\Theta(2u_1 + q_1) + \eta_i \phi_1] + 2ik^2\phi_1 T_h = 0, \quad (59)$$

$$\partial_t T_h - 4k^2 \text{Im}(\phi_1^* T_1) = 0, \quad (60)$$

where $[n_1(t), u_1(t), T_1(t), q_1(t)] = \int_{-\infty}^{\infty} dv_{\parallel} f_1(v_{\parallel}, t) [1, v_{\parallel}, (v_{\parallel}^2 - 1), (v_{\parallel}^3 - 3v_{\parallel})]$ and $[u_h(t), T_h(t)] = \int_{-\infty}^{\infty} dv_{\parallel} h(v_{\parallel}, t) \times [v_{\parallel}, (v_{\parallel}^2 - 1)]$. We also obtain from Eq. (48)

$$n_1 = \phi_1. \quad (61)$$

Here, we should note that $\phi_h(t) = n_h(t) \equiv \int_{-\infty}^{\infty} dv_{\parallel} h(v_{\parallel}, t) = 0$. The entropy balance equation similar to Eq. (39) is derived from Eqs. (56)–(61) as

$$\frac{d}{dt} \left(\frac{1}{2} |n_1|^2 + \frac{1}{2} |u_1|^2 + \frac{1}{4} |u_h|^2 + \frac{1}{4} |T_1|^2 + \frac{1}{8} |T_h|^2 + \frac{1}{2} |\phi_1|^2 \right) = \eta_i q_x + \text{Re} \left(\frac{T_1}{2} ik\Theta q_1^* \right), \quad (62)$$

where $q_x \equiv \text{Re}(\frac{1}{2} T_1 ik\phi_1^*)$ is the heat flux in the x direction. Comparing Eq. (62) to Eq. (50) and using the Hermite-polynomial expansion similar to Eq. (37), we obtain

$$\text{Re} \left(\frac{T_1}{2} ik\Theta q_1^* \right) = - \frac{d}{dt} \left(\frac{1}{12} |q_1|^2 + \frac{1}{24} |q_h|^2 + \dots \right), \quad (63)$$

where \dots represents the high-order-moment terms corresponding to $\sum_{n \geq 4} (n!/2) |\varphi_{nk}|^2$ in Eq. (40). For the case of the exact solution shown in Sec. III A, the time average of the left-hand side of Eq. (62) and that of the right-hand side of Eq. (63) vanish and accordingly the time average of the heat flux q_x vanishes. Thus, it is not practical to consider

the three-mode ITG system for estimating the anomalous heat diffusivity in the steady turbulent state, although it is a useful nonlinear system for examining the validity of kinetic-fluid closure models. There exists another simple set of fluid equations, which is used to evaluate the anomalous heat diffusivity due to the toroidal ITG mode.²⁴

Now, let us apply the NCM presented in Eq. (25) and put

$$q_1 = C_{T1}T_1 + C_{u1}u_1 + C_{n1}n_1, \tag{64}$$

where C_{T1} , C_{u1} , and C_{n1} are real coefficients given from Eqs. (28) and (29) as

$$C_{T1} = C_{Lr1} - C_{Li1} \frac{\text{Re}(\xi_1 \zeta_1^*)}{\text{Im}(\xi_1 \zeta_1^*)} - C_{n1} \frac{\xi_{i1}}{\text{Im}(\xi_1 \zeta_1^*)}, \tag{65}$$

$$C_{u1} = C_{Li1} \frac{|\zeta_1|^2}{\text{Im}(\xi_1 \zeta_1^*)} + C_{n1} \frac{\zeta_{i1}}{\text{Im}(\xi_1 \zeta_1^*)}, \tag{66}$$

$$C_{n1} = 0. \tag{67}$$

Here, $C_{L1} \equiv C_{L1r} + iC_{L1i} \equiv B(\omega_{L1}/k\Theta)$, $\xi_1 \equiv \xi_{r1} + i\xi_{i1} \equiv (\omega_{L1} - k)/(k\Theta)$, and $\zeta_1 \equiv \zeta_{r1} + i\zeta_{i1} \equiv \omega_{L1}(\omega_{L1} - k)/(k\Theta)^2 - 2$. The complex-valued eigenfrequency ω_{L1} is determined by the dispersion relation $D(\omega_{L1}) \equiv 1 - \int dv_{\parallel} kG(v_{\parallel})/(\omega_{L1} - k\Theta v_{\parallel}) = 0$ and $\text{Im}(\omega_{L1}) > 0$ is assumed.

Equations (56)–(61) with the NCM given by Eqs. (64)–(67) form a closed system of fluid equations for the three-mode ITG system. Figures 2(a) and 2(b) show $|\phi_1(t)|$ and $\text{Re}[\phi_1(t)/|\phi_1(t)|]$, respectively, which are obtained by numerically solving these fluid equations. A nondissipative time integration scheme¹⁴ is employed for these numerical calculations. Here, $k=0.1$, $\Theta=1$, and $\eta_i=10$ are used. For this case, we have $C_{L1} = -0.381 - 1.186i$, $C_{T1} = -2.878 \times 10^{-2}$ and $C_{u1} = 1.477$ with $C_{n1} = 0$. The initial conditions are $n_1(0) = \phi_1(0) = 0.01$, $u_1(0) = -2.149 \times n_1(0)$, $T_1(0) = -0.220 \times n_1(0)$, and $u_h(0) = t_h(0) = 0$, which are consistent with the initial conditions $[a(0), b(0), c(0)] = (0.01, 0, 0)$ for the WSS solution in Eq. (51) (the same initial conditions as used in Fig. 1). The fluid equations in Eqs. (56)–(61) can reproduce the WSS exact nonlinear solution since the NCM given by Eqs. (64)–(67) is completely satisfied by the WSS solution. It is noted that the WSS solution can be reproduced by the closure relation given by Eqs. (64)–(66) even with an arbitrary nonzero real value given to C_{n1} as shown in Appendix B. Also, it can be shown in Appendix B that, even if Eqs. (65)–(67) are not satisfied, the closure relation in Eq. (64) with real-valued coefficients C_{T1} , C_{u1} , and C_{n1} can give the WSS-type double-periodic nonlinear solution, which consists of the normal mode and its complex conjugate, since the time reversibility is still retained. For example, the case of the most simple closure, in which $q_1 = 0$ ($C_{T1} = C_{u1} = C_{n1} = 0$), and that of the Hammett–Perkins closure $q_1 = -2(2/\pi)^{1/2} ik\Theta T_1$ are plotted for comparison to the WSS solution in Fig. 2. The time evolution of the potential for the $q_1 = 0$ case shows a qualitatively better agreement with the exact solution than for the Hammett–Perkins model. In the Hammett–Perkins model, the potential $|\phi_1(t)|$ is saturated at a certain amplitude,

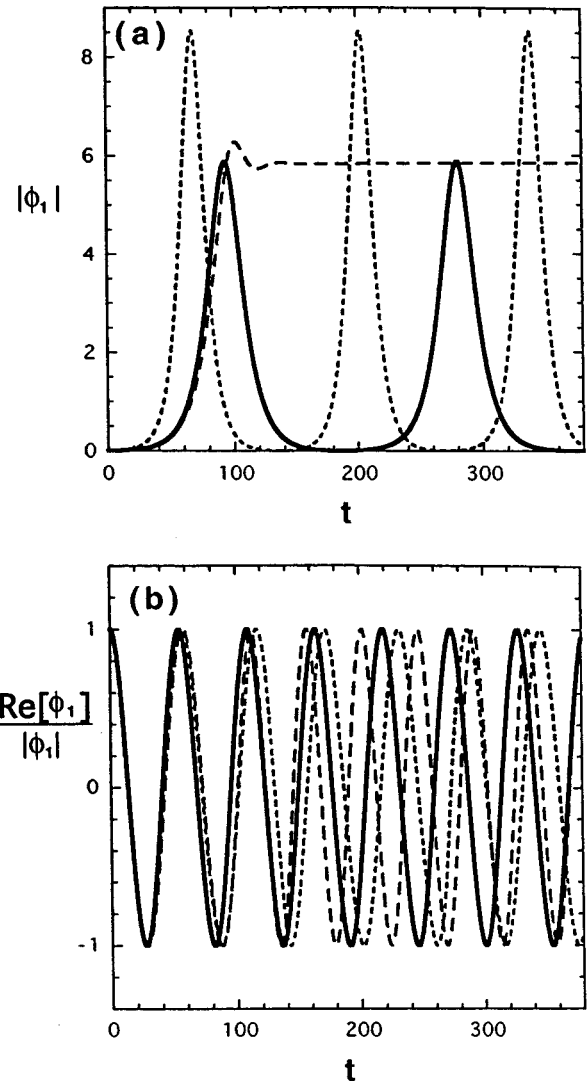


FIG. 2. Numerical solutions of the fluid system of Eqs. (56)–(61) and (64) for $k=0.1$, $\Theta=1$, $\eta_i=10$, $C_{T1} = -2.878 \times 10^{-2}$, $C_{u1} = 1.477$ and $C_{n1} = 0$. The initial conditions are given by $n_1(0) = \phi_1(0) = 0.01$, $u_1(0) = -2.149 \times n_1(0)$, $T_1(0) = -0.220 \times n_1(0)$, and $u_h(0) = t_h(0) = 0$, which are consistent with the initial conditions used for the WSS exact kinetic solution in Fig. 1. Solid curves in (a) and (b) represent $|\phi_1(t)|$ and $\text{Re}[\phi_1(t)/|\phi_1(t)|]$, respectively, obtained by using the NCM in Eqs. (64)–(67) and completely agree with those of the WSS exact kinetic solution. Results obtained by using the Hammett–Perkins model and the $q_1=0$ model are also shown by dashed and dotted curves, respectively.

which is in contrast to the periodic amplitude oscillation shown by the exact solution. Also, in the Hammett–Perkins model, the time average of the heat flux q_x in the three-mode ITG system takes on an artificial nonzero value since $\eta_i \bar{q}_x = -\text{Re}(\frac{1}{2} T_1 ik \Theta q_1^*) = (2/\pi)^{1/2} (k\Theta)^2 |T_1|^2 > 0$. This \bar{q}_x follows from the entropy balance equation (62) with $q_1 = -2(2/\pi)^{1/2} ik \Theta T_1$ where $\bar{\cdot}$ represents the time average.

Next, we compare solutions of the fluid equations with kinetic solutions for the case in which initial conditions are inconsistent with the WSS solution. The simplest example of such initial conditions is given by the Maxwellian form of the initial distribution function $f_1(v_{\parallel}, t=0) \propto e^{-v_{\parallel}^2/2}/(2\pi)^{1/2}$. Figures 3(a) and 3(b) show $|\phi_1(t)|$ and $\text{Re}[\phi_1(t)/|\phi_1(t)|]$, respectively, which are obtained by nu-

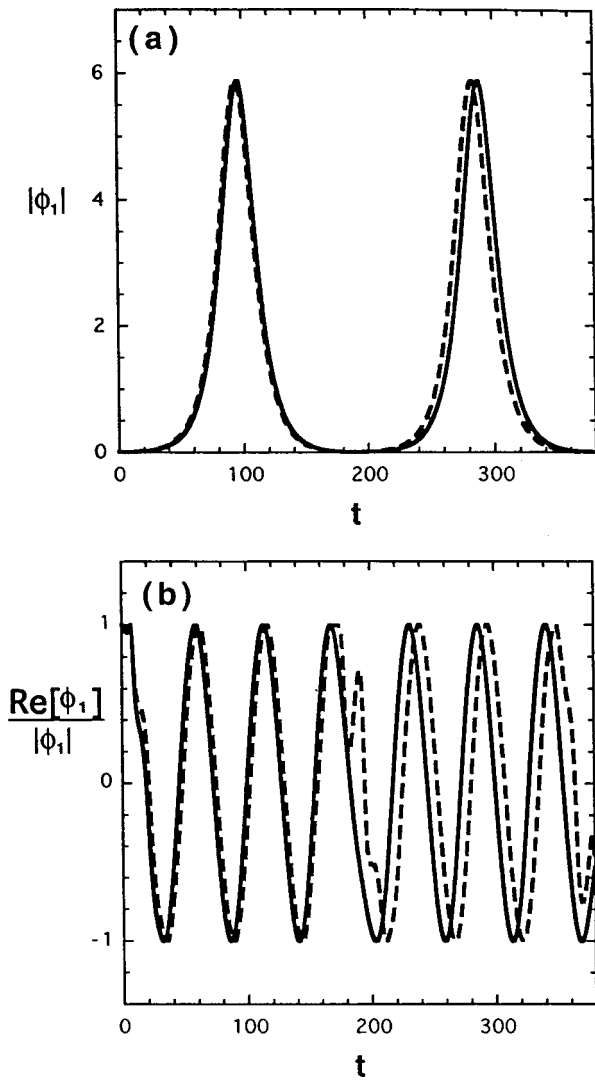


FIG. 3. Comparison between kinetic and fluid solutions. Solid curves in (a) and (b) represent $|\phi_1(t)|$ and $\text{Re}[\phi_1(t)/\phi_1(t)]$, respectively, obtained by numerically solving the kinetic system of Eqs. (46)–(48) for $k=0.1$, $\Theta=1$, and $\eta_i=10$ with the initial conditions $f_1(v_{\parallel},0)=0.01 \times e^{-v_{\parallel}^2/2}/(2\pi)^{1/2}$ and $h(v_{\parallel},0)=0$. Dashed curves represent results obtained by numerically solving the fluid system of Eqs. (56)–(61) with the NCM in Eqs. (64)–(67) for the initial conditions $n_1(0)=\phi_1(0)=0.01$ and $u_1(0)=T_1(0)=u_h(0)=t_h(0)=0$.

merically solving Eqs. (46)–(48) for $k=0.1$, $\Theta=1$, and $\eta_i=10$ with the initial conditions $f_1(v_{\parallel},0)=n(0)e^{-v_{\parallel}^2/2}/(2\pi)^{1/2}$ [$n(0)=0.01$] and $h(v_{\parallel},0)=0$. These initial conditions are the same as used in the kinetic simulations in Ref. 14. Results obtained by numerically solving Eqs. (56)–(61) and (64)–(67) for the initial conditions $n_1(0)=\phi_1(0)=0.01$ and $u_1(0)=T_1(0)=u_h(0)=t_h(0)=0$ are also plotted in Figs. 3(a) and 3(b) for comparison to the kinetic solution. Kinetic and fluid results for this case are in a good agreement except that a small potential phase deviation appears after the potential amplitude recurs to the low level of the initial condition.

Figure 4 shows the period T of the potential amplitude $|\phi_1(t)|$ ($=|n_1(t)|$) as a function of the initial amplitude $|\phi_1(0)|$ ($=|n_1(0)|$) for the case of $k=0.1$, $\Theta=1$, $\eta_i=10$,

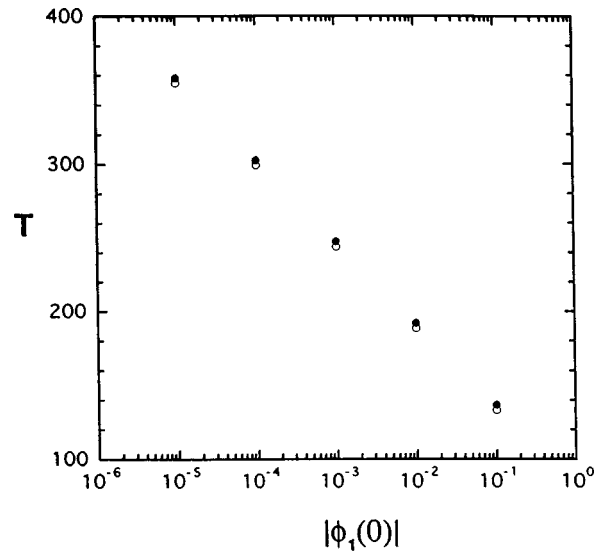


FIG. 4. Period T of the potential amplitude $|\phi_1(t)|$ as a function of the initial amplitude $|\phi_1(0)|$. Here, $k=0.1$, $\Theta=1$, $\eta_i=10$, $f_1(v_{\parallel},0)=n_1(0)e^{-v_{\parallel}^2/2}/(2\pi)^{1/2}$ [$n_1(0)=\phi_1(0)$], and $h(v_{\parallel},0)=0$. Solid and open circles represent results from solving the kinetic system of Eqs. (46)–(48) and those from solving the fluid system of Eqs. (56)–(61) with the NCM in Eqs. (64)–(67), respectively.

$f_1(v_{\parallel},0)=n_1(0)e^{-v_{\parallel}^2/2}/(2\pi)^{1/2}$, and $h(v_{\parallel},0)=0$. We see that the period T is proportional to $\log[1/|\phi_1(0)|]$ as predicted from the WSS solution in Ref. 14. In Fig. 4, results from numerical solutions of the fluid equations (56)–(61) and of the kinetic equations (46)–(48) are both plotted. We find that this kinetically closed fluid model accurately reproduces the initial-value dependence of the period of the amplitude oscillation.

IV. CONCLUSIONS

In the present paper, we have presented a new nondissipative closure model (NCM). We have shown that both linearly unstable modes and their complex conjugate are exact solutions of the linearized version of the collisionless kinetic equation with time reversibility. In order to take account of the nondissipative nature of the kinetic equation, the NCM is derived such that the relation between the fluctuations in the parallel heat flux, the temperature, and the parallel flow is valid both for linearly unstable normal modes and their complex conjugate as well as for any linear combination of them. The fluctuations obtained by the complex conjugate of the linearly stable modes are no longer linear solutions. For the linearly stable modes, we use the dissipative closure relation, which reduces to previous closure models by Hammett and Perkins,¹⁰ and by Chang and Callen¹¹ in limiting cases.

Kinetic and fluid entropy balances for the collisionless system are investigated to compare effects of the NCM and the Hammett–Perkins model on the entropy production, the turbulence saturation, and the anomalous perpendicular heat transport. The quasisteady state for the collisionless turbulent plasma is defined as the state in which the amplitudes of fluid variables corresponding to low-order velocity moments of the distribution function saturate but the high-order moments

and accordingly the total entropy grow indefinitely in time. The entropy production rate given by the product of the perpendicular heat flux and the temperature gradient balance with the correlation between the parallel heat flux and temperature fluctuations in the quasisteady state. In the NCM, this correlation function takes the nondissipative form in the unstable wave number region while, in the Hammett–Perkins model, it is written as a dissipation proportional to the square of the temperature fluctuation amplitude for all wave number regions. Then, it is expected that, when used in turbulence simulations, the NCM predicts different results on the entropy production rate and the anomalous heat transport from those given by the Hammett–Perkins and other dissipative closure models.

The NCM is applied to the three-mode ITG problem as an example. The WSS exact nonlinear kinetic solution can be reproduced from the fluid system of equations with the NCM. Other numerical kinetic solutions can also be accurately described by the fluid system. Especially the oscillatory behaviors of the potential amplitude and the dependence of the oscillation period on the initial amplitude, which cannot be treated by the conventional dissipative closure models, are well reproduced by the NCM. While the three-mode ITG problem is an interesting and successful nonlinear test case, one might wonder whether the NCM also works well for more realistic many-mode turbulent cases which significantly differ from the three-mode case in some aspects. The three-mode system involves interaction between only a single coherent eddy of the (1,1)-mode and a background profile flattening of the (2,0)-mode, and shows fairly regular periodic behavior as given by the exact solution in Eq. (51). However, the behavior of nonintegrable chaotic systems such as many-mode turbulent systems is very different from such a regular one, and the validity of the use of a nondissipative or a dissipative closure depending on the linear growth rate criterion should be checked for such fully turbulent cases. (Note that even the fluid system using linear closure models can be highly nonlinear and turbulent because of the $\mathbf{E} \times \mathbf{B}$ convection terms although it does not necessarily imply the correct description of the original turbulent kinetic system by the fluid model.) Another point to clarify is collisional effects on the closure. Collisions are necessary for true steady-state turbulence of kinetic systems to be realized, and even a small amount of collisions may have significant effects. In order to investigate the subjects discussed above, applications of the NCM to systems with a higher number of degrees of freedom is work currently in progress.

ACKNOWLEDGMENTS

Part of this work was completed when one of the authors (H.S.) was an exchange scientist at the Institute for Fusion Studies, the University of Texas at Austin, under the Joint Institute for Fusion Theory, U.S.-Japan Fusion Cooperation Program. Numerical computations of the kinetic equations are performed on the NIFS MISSION System (Man-Machine Interactive System for Simulation). This work is supported in part by the Grant-in-Aid from the Japanese Ministry of Education, Science, Sports, and Culture, No. 12680497.

APPENDIX A: HAMILTONIAN REPRESENTATION OF EQS. (52) AND (55)

Here, it is shown that Eqs. (52) and (55) can be written in the Hamiltonian form. First, we easily find from Eqs. (52) that $C_1 \equiv c(t) - (2k^2/\gamma)a^2(t)$ is a constant of the motion. Then, substituting $c = C_1 + (2k^2/\gamma)a^2$ into the equations for time evolution of a and b , we obtain the Hamiltonian equations of motion

$$\frac{da}{dt} = \frac{\partial H(a,b)}{\partial b}, \quad \frac{db}{dt} = -\frac{\partial H(a,b)}{\partial a}, \tag{A1}$$

where (a,b) are regarded as canonical variables and the Hamiltonian is given by

$$H(a,b) = \frac{\gamma}{2}b^2 + \left(-\frac{\gamma}{2} + k^2C_1\right)a^2 + \frac{k^4}{\gamma}a^4. \tag{A2}$$

Here, the Hamiltonian $H(a,b)$ has no explicit dependence on time and accordingly is a constant of motion. Therefore, this Hamiltonian system is integrable. With b playing the role of momentum, the quadrature $H = E = \text{const}$ gives an elliptic integral and the solutions for $a(t)$, $b(t)$, and $c(t)$, which are periodic functions of time, are found in Ref. 14.

Similarly, Eqs. (55) can be written as the Hamiltonian equations

$$\frac{d\alpha^<}{dt} = \frac{\partial \mathcal{H}(\alpha^<, \alpha^>)}{\partial \alpha^>}, \quad \frac{d\alpha^>}{dt} = -\frac{\partial \mathcal{H}(\alpha^<, \alpha^>)}{\partial \alpha^<}, \tag{A3}$$

where $(\alpha^<, \alpha^>)$ are regarded as canonical variables and the Hamiltonian is given by

$$\begin{aligned} \mathcal{H}(\alpha^<, \alpha^>) = \frac{1}{2}H = & -\gamma\alpha^>\alpha^< + \frac{k^2C_1}{2}(\alpha^> + \alpha^<)^2 \\ & + \frac{k^4}{2\gamma}(\alpha^> + \alpha^<)^4. \end{aligned} \tag{A4}$$

APPENDIX B: EXACT SOLUTION OF FLUID EQUATIONS

Here, we consider a system of fluid equations consisting of Eqs. (56)–(61) and (64). First, we only assume the coefficients C_{T1} , C_{u1} , and C_{n1} in Eq. (64) to be real constants without imposing the conditions in Eqs. (65)–(67) on them. Let us consider the solutions of the fluid equations which are written as

$$\begin{aligned} n_1(t) &= [a(t)n_{Lr} + ib(t)n_{Li}] \exp(-i\omega_{Lr}t) \\ &= [\alpha^>(t)n_L + \alpha^<(t)n_L^*] \exp(-i\omega_{Lr}t), \\ u_1(t) &= [a(t)u_{Lr} + ib(t)u_{Li}] \exp(-i\omega_{Lr}t) \\ &= [\alpha^>(t)u_L + \alpha^<(t)u_L^*] \exp(-i\omega_{Lr}t), \\ T_1(t) &= [a(t)T_{Lr} + ib(t)T_{Li}] \exp(-i\omega_{Lr}t) \\ &= [\alpha^>(t)T_L + \alpha^<(t)T_L^*] \exp(-i\omega_{Lr}t), \\ u_h(t) &= c(t)u_{Li}, \quad T_h(t) = c(t)T_{Li}, \quad \phi_1(t) = n_1(t), \end{aligned} \tag{B1}$$

where $\alpha^> = \frac{1}{2}(a+b)$, $\alpha^< = \frac{1}{2}(a-b)$, a and b are real functions of time, and the complex constants $n_L = n_{Lr} + in_{Li}$, $u_L = u_{Lr} + iu_{Li}$, $T_L = T_{Lr} + iT_{Li}$, and $\omega_L = \omega_{Lr} + i\gamma$ are determined from

$$\begin{aligned}\omega_L n_L &= k(\Theta u_L + \phi_L), \\ \omega_L u_L &= k\Theta(n_L + T_L + \phi_L), \\ \omega_L T_L &= k[\Theta(2u_L + q_L) + \eta_i \phi_L], \\ n_L &= \phi_L = 1 \quad (\text{normalization}), \\ q_L &= C_{T1} T_L + C_{u1} u_L + C_{n1} n_L.\end{aligned}\tag{B2}$$

Here, the complex eigenfrequency $\omega_L = \omega_{Lr} + i\gamma$ is given from Eqs. (B2) as a solution of the cubic algebraic equation with $\gamma > 0$.

Substituting Eqs. (B1) into Eqs. (56)–(60), we find that $a(t)$, $b(t)$, and $c(t)$ should satisfy

$$\begin{aligned}da/dt &= \gamma b, \\ db/dt &= \gamma a - 2k^2 ac, \\ dc/dt &= 4k^2 ab,\end{aligned}\tag{B3}$$

which are the same as Eqs. (52) for the WSS kinetic solution. From Eqs. (53) and (B3), the same equations as Eqs. (55) for $\alpha^>(t)$, $\alpha^<(t)$, and $c(t)$ are also derived. Now, it turns out that a WSS-type double-periodic solution given by Eqs. (B1)–(B3) appears from this system of fluid equations.

Furthermore, when imposing the conditions in Eqs. (65) and (66) on the real coefficients C_{T1} , C_{u1} , and C_{n1} [Eq. (67) is not necessary], the complex eigenfrequency $\omega_L = \omega_{Lr} + i\gamma$ also coincides with that given by the kinetic dispersion relation. Then, the system of fluid equations includes the

WSS solution as one of their solutions. In other words, the exact kinetic solution of the three-mode ITG problem can be reproduced by the fluid equations with a proper collisionless closure model.

¹W. Horton, Rev. Mod. Phys. **71**, 735 (1999).

²W. W. Lee and W. M. Tang, Phys. Fluids **31**, 612 (1988).

³S. E. Parker, W. W. Lee, and R. A. Santoro, Phys. Rev. Lett. **71**, 2042 (1993).

⁴A. M. Dimits, T. J. Williams, J. A. Byers, and B. I. Cohen, Phys. Rev. Lett. **77**, 71 (1996).

⁵Z. Lin, T. S. Hahm, W. W. Lee, W. M. Tang, and R. B. White, Science **281**, 1835 (1998).

⁶W. Dorland and G. W. Hammett, Phys. Fluids B **5**, 812 (1993).

⁷R. E. Waltz, G. D. Kerbel, and J. Milovich, Phys. Plasmas **1**, 2229 (1994).

⁸M. Kotschenreuther, W. Dorland, M. A. Beer, and G. W. Hammett, Phys. Plasmas **2**, 2381 (1995).

⁹M. A. Beer, G. W. Hammett, G. Rewoldt, E. J. Synakowski, M. C. Zarnstorff, and W. Dorland, Phys. Plasmas **4**, 1792 (1997).

¹⁰G. W. Hammett and F. W. Perkins, Phys. Rev. Lett. **64**, 3019 (1990).

¹¹Z. Chang and J. D. Callen, Phys. Fluids B **4**, 1167 (1992).

¹²S. E. Parker, W. Dorland, R. A. Santoro, M. A. Beer, Q. P. Liu, W. W. Lee, and G. W. Hammett, Phys. Plasmas **1**, 1461 (1994).

¹³A. M. Dimits, G. Bateman, M. A. Beer *et al.*, Phys. Plasmas **7**, 969 (2000).

¹⁴T.-H. Watanabe, H. Sugama, and T. Sato, Phys. Plasmas **7**, 984 (2000).

¹⁵N. Mattor and S. E. Parker, Phys. Rev. Lett. **79**, 3419 (1997).

¹⁶N. Mattor, Phys. Plasmas **5**, 1822 (1998).

¹⁷N. Mattor, Phys. Plasmas **6**, 1059 (1999).

¹⁸N. Mattor, Phys. Plasmas **6**, 1065 (1999).

¹⁹J. A. Krommes and G. Hu, Phys. Plasmas **1**, 3211 (1994).

²⁰H. Sugama and W. Horton, Phys. Plasmas **2**, 2989 (1995).

²¹H. Sugama, M. Okamoto, W. Horton, and M. Wakatani, Phys. Plasmas **3**, 2379 (1996).

²²G. W. Hammett, M. A. Beer, W. Dorland, S. C. Cowley, and S. A. Smith, Plasma Phys. Controlled Fusion **35**, 973 (1993).

²³B. N. Rogers, W. Dorland, and M. Kotschenreuther, Phys. Rev. Lett. **85**, 5336 (2000).

²⁴W. Horton, Plasma Phys. **23**, 1107 (1981).